Elastic constants and thermophysical properties of CuPd: First-principles study

A. Benmakhlouf[a], S. Daoud[a], N. Bouarissa[b,*], and O. Allaoui[c]

[a]*Laboratoire de Génie des Procédés, Université Amar Telidji de Laghouat, Algérie.*
Laboratoire Matériaux et Systèmes Electroniques, Université Mohamed El Bachir El Ibrahimi, Algérie.
[b]*Laboratory of Materials Physics and its Applications, University of M'sila, Algeria.*
[*]*e-mail: n_bouarissa@yahoo.fr*
[c]*Laboratoire de Génie des Procédés, Université Amar Telidji de Laghouat, Algérie.*

Received 26 August 2023; accepted 3 September 2024

Based on density functional theory, the structural parameters, elastic moduli, and thermophysical properties of Copper-palladium (CuPd) inter-metallic compound at various temperatures and under high pressures have been studied using first-principles calculations. The pseudopotential-plane wave method within the generalized gradient approximation approach was utilized. The material considered is a pure substance of solid CuPd arranged in the body-centered cubic fashion. Our results show a lattice constant of around 3.001 Å, in good agreement with the experimental value of 2.96 Å from literature. The elastic stiffness constants increase monotonically with pressure. Mechanical stability, isothermal bulk modulus, heat capacity, Debye temperature, and entropy are also analyzed for pressures from 0 to 12 GPa and temperatures from 0 to 600 K. At room temperature and zero-pressure, the constant volume heat capacity and the entropy are found to be 45.65 and 53.94 J/mol.K, respectively.

Keywords: Copper-palladium; mechanical properties; thermal properties; high temperature; high-pressure.

DOI: https://doi.org/10.31349/RevMexFis.71.020501

1. Introduction

Copper-palladium with the chemical formula CuPd, and copper scandium with the chemical formula CuSc are two renowned members of 'd' block transition metal family. These two compounds are complex with their boiling points and high melting temperature [1]. The transition metal CuX (X = Sc and Pd) intermetallic compounds own many promising mechanical and physical properties such as high tensile strength, good ductility, high corrosion resistance, large mechanical stability under compression, and high thermal stability [1, 2].

The elastic and thermodynamic properties of solid materials are important for the understanding of the physics of the solid state matter [3–6]. This is due to their direct relationship with other fundamental properties of matter. At extreme conditions of pressure and temperature, the fundamental properties of solid materials may behave differently [7–12]. The knowledge of the behavior of these properties under high pressure and temperature is very useful for our understanding of fundamental properties of materials subjected to severe conditions and for technological applications. As a matter of fact, pressure and temperature are attractive thermodynamical variables that allows a variation in the fundamental properties of solid materials when the inter-atomic distances are changed in a systematic way [13–16]. Almost, copper-based binary compounds were the object of several studies on their fundamental properties in the last two decades. In fact, a lot of theoretical calculations [1, 2, 17–20] and experimental studies [21] have been performed on structural parameters, elastic constants, and thermophysical properties at ambient conditions and under high pressure and temperature on CuX (X = Sc and Pd) intermetallic compounds in the eightfold coordinated CsCl-type structure (B2).

Like silver, pure copper has also a high electrical conductivity. At 20°C, it has an electrical conductivity of around 5.98×10^7 S.m^{-1} Palladium, a member of the platinum group of metals, is the least dense element in this group. Its electrical conductivity is slightly lower than that of copper, approximately 9.28×10^6 S.m^{-1} at 20°C [22]. In the CsCl-type (B2) structure, the CuX (X = Sc and Pd) intermetallic compounds crystallize with Cu atoms located at the vertices and Sc (Pd) atom in the center of body-centered cubic cell [1, 2].

In the present work, we report on first-principles calculations of the equation of state (EoS), structural parameters, mechanical properties and the influence of pressure and temperature on several thermodynamic quantities of CuPd intermetallic compound in its metallic solid CsCl-type (B2) structure using the pseudopotential plane wave method in the framework of the density functional theory (DFT) [23, 24].

2. Methods

The calculations reported in the present work have been performed within the DFT using pseudopotential-plane wave ($PP-PW$) method. The static energy-volume (E, V) data and the elastic constants C_{ij} are obtained using the CASTEP code [25]. For the exchange-correlation potential, the generalized gradient approximation (GGA) for the total energy calculations in the form proposed by Perdew-Burke-Ernzerhof (PBE) [26] scheme is employed for electron-electron interaction. In order to reduce the required number of plane waves, chemically inactive core electrons are effectively replaced with an ultra-soft pseudopotential [27].

The plane-wave basis set cut-off energy used in the present calculations is taken as 500 eV. The Monkhorst-Pack method [28] with a $16 \times 16 \times 16$ special k-point mesh is used to realize the special points sampling integration over the Brillouin zone. To minimize the total energy, interatomic forces and unit-cell stress, the lattice parameter has been independently modified. For the geometry optimization, the difference within 5×10^{-6} eV/atom in the total energy is taken, the maximum stress is taken to be 0.02 GPa, maximum ionic displacement within 5×10^{-4} Å, and a maximum ionic Hellmann-Feynman force within 0.01 eV/Å.

In order to obtain the pressure and temperature dependence of the thermodynamic properties of CuPd intermetallic compound, the quasi-harmonic Debye model is successfully applied; our calculations are implemented through the Gibbs code [29]. The method of the calculation adopted in the present work and the different relationships used here are detailed elsewhere [2, 29].

3. Results and discussion

3.1. Structural parameters at equilibrium

The total energy of the material of interest (CuPd with CsCl-type structure) has been calculated as a function of the unit-cell volume around the equilibrium cell volume V_0, using the GGA scheme, to determine the equilibrium structural parameters (the equilibrium lattice constant a_0, bulk modulus B_0, and its first pressure derivative B_0'). Then the calculated total energies were minimized by means of Murnaghan's equation of state [30], as shown in Fig. 1. Our obtained values of the lattice parameter at equilibrium a_0, bulk modulus B_0, and its pressure derivative B_0' are also summarized in Table I, and compared with other theoretical results [1, 17, 18] and experimental data [21]. From the results summarized in Table I, it can be observed that our result of a_0 of the material of interest is in good agreement with the theoretical one of 2.995 Å [18], and the experimental one of 2.96 Å [21]. Our obtained value (3.001 Å) is overestimated with respect to that of experiment (2.96 Å) [21] by less than 1.4%. Our calculated value of the bulk modulus B_0 and its pressure derivative B_0' are also in good agreement compared to the theoretical ones [1, 3]. Our obtained value of 160.04 GPa of B_0 is almost equal to the theoretical one of 160.37 GPa obtained by Baranov [17] and our obtained value (5.26) of B_0' is underestimated with respect to the theoretical one of 5.33 [1] by less than 1.32%.

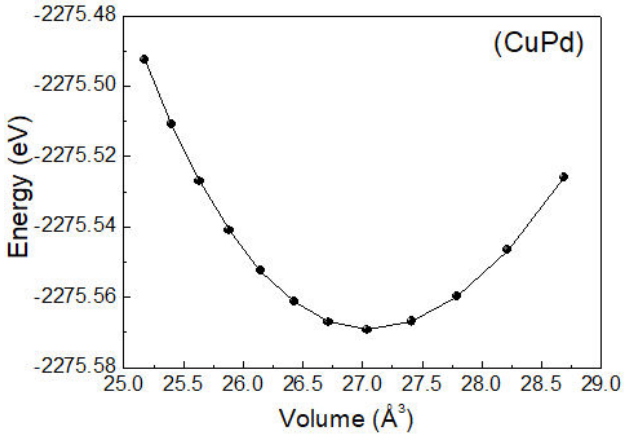

FIGURE 1. Total energy versus the volume for CuPd intermetallic compound.

3.2. Mechanical properties

3.2.1. *Elastic constants and some other derivative quantities*

Due to the symmetry elements in the crystal, there are only three independent elastic stiffness constants (C_{11}, C_{12} and C_{44}) in the case of cubic crystals [2]. At zero-pressure, the evaluated elastic constants C_{ij} of CuPd intermetallic compound in cubic CsCl-type structure are presented in Table II, and compared with other theoretical data [1]. From Table II, we observe that our calculated elastic constants C_{ij} are in reasonably good agreement with the previous theoretical data reported in Ref. [1]. At zero-pressure, the calculated elastic constants C_{ij} of CuPd intermetallic compound satisfy the requirement mechanical stability criterions, which are given as [1, 31]

$$C_{11} + 2C_{12} > 0, C_{11} - C_{12} > 0, C_{44} > 0, \quad \text{and} \quad C_{11} > B > C_{12}, \tag{1}$$

in Eq. (1) means that the bulk modulus B, the shear modulus C=C_{44} and the tetragonal shear modulus C'=$(C_{11} - C_{12})/2$ must be positive. The tetragonal shear modulus measures the response of a crystal to volume-conserving tetragonal shear

TABLE I.

Parameter	Our work	Other works
a_0 (Å)	3.002	3.0145[a,e], 2.9663[a,f], 2.956[a,g] 2.961[b], 2.995[c], 2.96[d]
B_0 (GPa)	160.04	158.85[a,e], 184.92[a,f], 188.84[a,g], 160.37[d]
B_0'	5.26	4.85[a,e], 4.71[a,f], 5.33[a,g]

TABLE II.

Parameter	Our work	Other works
C_{11}	181.07	184.03[a,b], 217.54[a,c], 208.66[a,d]
C_{122}	150.40	144.12[a,b], 173.72[a,c], 185.01[a,d]
C_{44}	97.10	60.87[a,b], 94.11[a,c], 69.47[a,d]

strain and can be linked with the stretching and the bending of atomic bonds [32].

It can be noticed that the C_{11} is slightly higher than C_{12}, while C_{44} is largely lower. This indicates that the velocity of a longitudinal wave in the $[100]$ direction is much larger than the shear wave as C_{11} is larger than C_{44}. This behavior of the elastic constants C_{ij} is also observed for zinc-blende zirconium carbide (ZrC) material [32].

The bulk modulus is defined as the reciprocal of the compressibility. A material that is difficult to compress has a large bulk modulus, but a small compressibility. When the bulk modulus is independent of pressure, this is a specific form of Hooke's law of elasticity. For crystals with cubic structure, the bulk modulus B and the elastic constants C_{ij} are related by [31]

$$B = (C_{11} + 2C_{12})/3. \tag{2}$$

At zero-pressure, the bulk modulus of CuPd intermetallic compound is found to be 160.62 GPa. It is also in reasonably good agreement with the previous theoretical data [1, 17]. Our obtained value deviates from the theoretical ones of 158.85 GPa reported by Jain *et al.* [1] and 160.37 GPa obtained by Baranov [17] by less than 1.12% and 0.16%, respectively.

Figure 2 shows the variations of the elastic constants C_{ij} and their aggregate bulk modulus B versus applied hydrostatic pressure for CuPd intermetallic compound. We observe a quasi-linear dependence in all curves. All parameters of interest increase monotonically with raising pressure.

The elastic constant C_{11} represents elasticity in length and a longitudinal strain produces a change in C_{11} [33]. On the other hand, the elastic constants C_{12} and C_{44} are related to the elasticity in shape, which representing a shear constant [33]. The best fit of our data regarding the elastic constants C_{ij}, and the bulk modulus B (in GPa) for CuPd obey the following expressions:

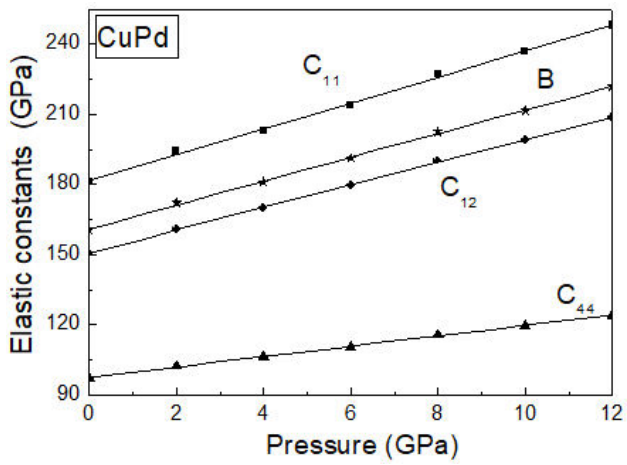

FIGURE 2. Variation of the elastic constants C_{ij} and the bulk modulus B as a function of the pressure.

$$C_{11} = 181.49 + 5.58p, \tag{3}$$

$$C_{12} = 150.95 + 4.81p, \tag{4}$$

$$C_{44} = 97.53 + 2.21p, \tag{5}$$

$$B = 161.13 + 5.07p. \tag{6}$$

The variation of the elastic constants C_{ij} as a function of pressure allowed us to predict the pressure derivatives $\partial C_{ij}/\partial P$. Our results regarding the pressure derivatives at zero-pressure: $\partial C_{11}/\partial P, \partial C_{12}/\partial P, \partial C_{44}/\partial P$ and $\partial B/\partial P$ of CuPd intermetallic compound are: 5.58, 4.81, 2.21 and 5.07, respectively. The results show that $\partial C_{44}/\partial P$ is the lowest value compared to other $\partial C_{ij}/\partial P$, thus indicates that the shear deformation designed by C_{44} parameter is less sensitive to the pressure than other parameters (C_{11}, C_{12} and B). It can be noted that the same behavior of the elastic constants C_{ij} under compression was also observed for CuSc intermetallic compound [2]. To the best of our knowledge, there is no data available in the literature on the pressure derivatives of elastic constants C_{ij} for the material of interest. For cubic crystals, a linear empirical expression linking the T_m to the elastic constant C_{11}, is given by [34, 35],

$$T_m = 553 + (591/Mbar)C_{11} \pm 300K. \tag{7}$$

Using the value of $C_{11} = 181.07$ GPa obtained at zero-pressure, the value of T_m of CuPd has been found to be 1623 ± 300 K. This value is much higher than the value of 872.6 ± 300 K of cubic zinc-blende copper iodide (CuI) semiconducting material [34]. To the best of our knowledge, there are no experimental or other theoretical data available so far to check the accuracy of our estimated Tm value of CuPd intermetallic compound with B2 structure.

On the macroscopic scale, the elastic moduli (Young modulus E, Poisson's ratio σ, etc.) were usually used to describe the elastic properties of solids. The Young's modulus E is a measure of the ability of solid material to defend longitudinal stress [36,37], while the Poisson's ratio σ is a measure of the Poisson effect; the phenomenon in which a material tends σ to expand (compress) in directions perpendicular to the direction of compression (expansion) [38]. For the aggregate polycrystalline materials (elements, compounds and alloys), the Young modulus E and Poisson's ratio σ are calculated as follows [36–38],

$$E = 9BG/(3B + G), \quad \text{and}$$
$$\sigma = (3B - 2G)/2(3B + G), \tag{8}$$

where B is the bulk modulus and G is the isotropic shear modulus. At equilibrium, our calculated values of G, E and σ are: 47.7 GPa, 130.21 GPa, and 0.365, respectively. They are presented in Table III, and compared with other available theoretical data of the literature [19]. It is seen also that, our calculated values of G, E and σ are in general in good agree-

TABLE III.

Pressure (GPa)	G (GPa)	E (GPa)	v	B/G	$E_{\max}/E_{\min}$	H_v (GPa)
0	47.70	130.21	0.365	3.37	5.44	3.57
1	38.97[a]	108.00[a]	0.386[a]	4.039[a]	-	-
2	50.77	138.66	0.366	3.39	5.29	3.70
4	51.75	141.75	0.369	3.50	5.62	3.62
6	54.00	148.06	0.371	3.54	5.58	3.68
8	57.05	156.47	0.371	3.55	5.42	3.82
10	58.74	161.29	0.373	3.60	5.47	3.83
12	61.13	167.95	0.374	3.63	5.45	3.91

ment with the previously calculated data [19], where for example, the value (0.365) of σ obtained in the present work deviates from the theoretical one of 0.386 reported by Jain *et al*. [19] by around 5.44%. It can be seen that CuPd has higher value of E compared to that (101.34 GPa) of CuSc [2], implying that the CuPd is more covalent in nature comparing to CuSc material [19]. Under compression our predicted values of the isotropic shear modulus G, the Young's modulus E, and the Poisson's ratio ν up to 12 GPa are also reported in Table III. All these different quantities increase monotonically with increasing pressure. The physical properties of solid materials are importantly related to the electronic configuration of molecules [39]. In this respect, the densities of states (DOSs) have been computed for CuPd in order to study the distribution of the electrons in different orbitals. Our results are displayed in Fig. 3. Note that the major contribution for the energy bands near the Fermi level of the CuPd crystal

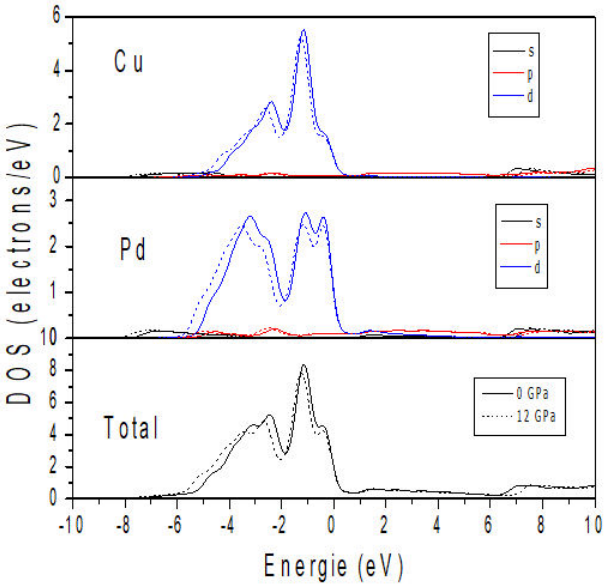

FIGURE 3. Total and local densities of states of CuPd intermetallic compound at equilibrium and 12 GPa.

comes from Cu-d and Pd-d electrons which play an important role in the conductibility of the crystal of interest. Upon compression of 12 GPa, we observe a shift of Cu-d and Pd-d electrons towards lower energies with respect to those at zero pressure. A useful visualization of the elastic anisotropy can be obtained by plotting a three-dimensional representation (3D) of the dependence of Young's modulus E on crystallographic direction in a crystal. For cubic crystals, the directional dependence of Young's modulus in *3D* representations can be given by the following relationship [40]

$$E(\overrightarrow{n}) = 1/[S_{11} - (2S_{11} - 2S_{12} - S_{44})({n_1}^2{n_2}^2 + {n_1}^2{n_3}^2 + {n_2}^2{n_3}^2)], \tag{9}$$

where S_{ij} design the elastic compliance constants, and n_1, n_2 and n_3 are the directional cosines to the x-, y- and z-axes, respectively. Equation (9) determines a 3D closed surface, and the distance from the origin of the system coordinates to this surface is equal to young's modulus in a given direction. For a perfectly isotropic material this surface would be a sphere, but often this is not the case even for cubic crystals [40]. Figures 4 and 5 show, respectively the three dimensional and the projections in 110 and 100 crystallographic planes of the Young's modulus of CuPd single material. At equilibrium, the estimated values $E_{\max}$ and $E_{\min}$ are along the [111] direction for 110 planes, and along [001] direction for 100 planes, respectively. The pressure dependence of $E_{\max}/E_{\min}$ is listed also in Table III. The variation of $E_{\max}/E_{\min}$ ratio as a function of pressure is not monotonic, reflecting the variation of the magnitude of the mechanical anisotropy under compression up to 12 GPa in CuPd intermetallic compound. In cubic crystals, the mechanical stability conditions on the elastic constants at any value of pressure are expressed as follows [2, 31]

$$\begin{aligned} K &= 1/3(C_{11} + 2C_{12} + P) > 0, \\ G &= 1/2(C_{11} - C_{12} - 2P) > 0, \quad \text{and} \\ G' &= (C_{44} - P) > 0. \end{aligned} \tag{10}$$

As pressure is applied to CuPd intermetallic compound with B2-type structure, it gets transformed from the ordered B2-type structure into another phase (perhaps to the disordered phase or to the amorphous state). The variation of the generalized elastic stability criteria G, G' and K are plotted against pressure in Fig. 6. From Fig. 6 in can be seen we found that G decreases gradually with increasing pressure and vanishes at about 26.5 GPa, which yields the phase transition pressure. Hardness is one of the basic mechanical properties of the solid. It represents the resistance to elastic and plastic deformation or brittle failure when compressive force is applied.

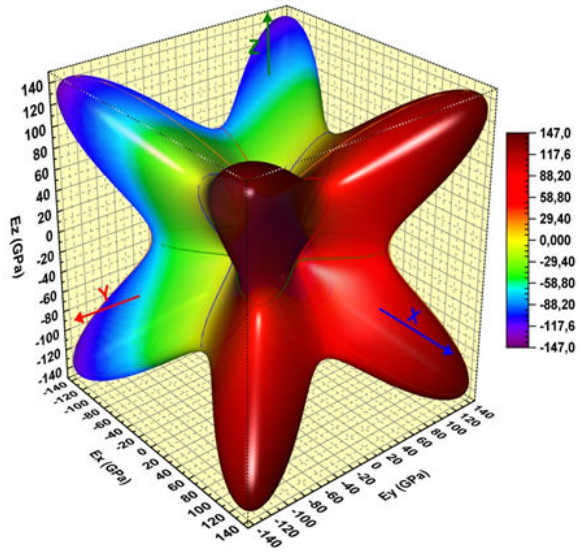

FIGURE 4. Graphical representation of the Young's modulus for CuPd material with B2 structure at equilibrium.

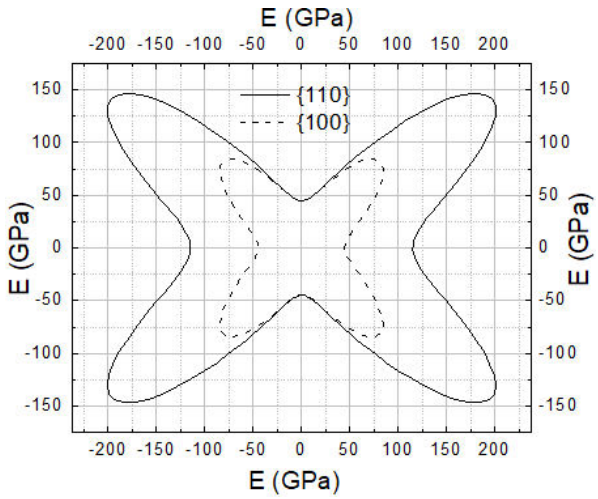

FIGURE 5. Variation of the generalized elastic stability criterions as a function of the pressure.

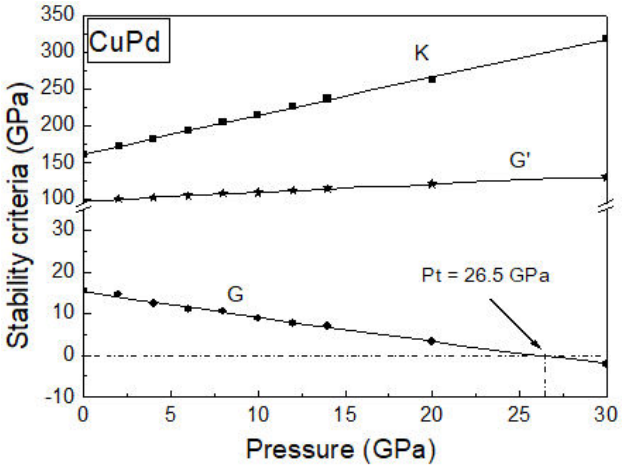

FIGURE 6. Longitudinal (v_l), transverse (v_t) and average (v_m) sound velocities of CuPd versus pressure.

The hardness of elements, compounds as well as alloys has a significant effect on their applications in functional materials [41]. The isotropic polycrystalline shear modulus is the most important parameter besides the bulk modulus for hardness of any material [32]. An empirical formula was usually used to predict the hardness of several compounds and alloys. This formula relates the Vickers hardness Hv and the elastic moduli; it is given as [42],

$$Hv = 0.92k^{1.137}G^{0.708}, \tag{11}$$

where the parameter k refers to the G/B ratio, B is the bulk modulus, and G is the shear modulus. Using our values of the modulus and the shear modulus obtained at zero-pressure, the predicted value of the Vickers hardness Hv of CuPd is 3.57 GPa. This value is lower than the hardness of the covalent materials, which are relatively high, in that the strong covalent bonds greatly hinder the plastic flow due to the pinned dislocation [41]. Under compression our predicted values of the Hv up to 12 GPa are reported in Table III. We can see that Hv of CuPd increases with raising pressure. To the best of our knowledge, there is no data available in the literature on the generalized elastic stability criteria and the Vickers hardness Hv for CuPd material with B2- structure. Hence, our result represents a prediction and may serve for a reference, and still await experimental and other theoretical confirmations.

3.2.2. *Sound velocity, Debye temperature and melting temperature*

From the theoretical elastic constants, we computed the elastic wave velocities. In this respect we have calculated the sound velocities and the Debye temperature using expressions from Refs. [2, 37] and presented them along with other results of Jain *et al.* [19] in Table IV. As can be seen from Table IV, our calculated values concerning the longitudinal (v_l), transverse (v_t) and average (v_m) sound velocities and the Debye temperature θ_D are in reasonable agreement with the previous theoretical data reported in Ref. [19], where for example our obtained value 2138 m/s of v_t overestimates the theoretical one (2078.34 m/s) [19] by only around 2.87%, while our value ($301K$) of θ_D overestimates the result ($291.49K$) [19] by only around 3.26%. The variation of the longitudinal (v_l), transverse (v_t) and average (v_m) sound velocities are drawn as functions of pressure in Fig. 7 for each compound of interest. It is inferred from Fig. 7 that all sound velocities increase monotonously with increasing pressure.

TABLE IV.

Parameter	Our work	Other works
v_l (m/s)	4635	4586.79[a]
v_t (m/s)	2138	2078.34[a]
v_m (m/s)	2408	2343.30[a]
θ_D (K)	301	291.49[a]

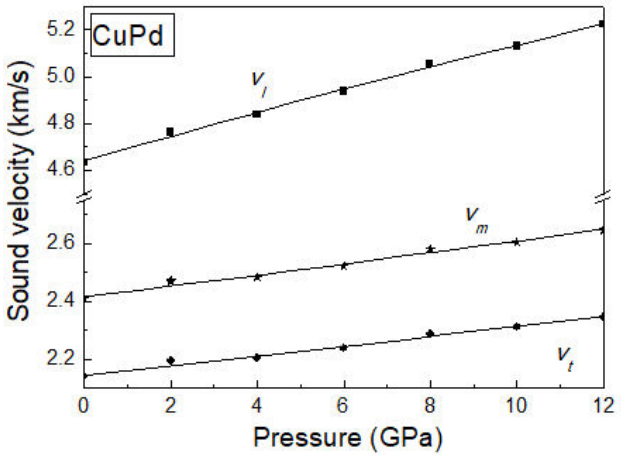

FIGURE 7. Variation of the unit cell volume as a function of the pressure at different temperatures.

This tendency of the sound velocities under compression was also obtained by Jain *et al*. [19] for CuPd compound. It can be noted that the same behavior of all sound velocities under pressure was also observed for CuSc intermetallic compound [2, 19].

3.3. Thermodynamic properties

As we mentioned below in Sec. 2, the pressure and temperature dependence of the thermodynamic properties of CuPd intermetallic compound were obtained from the quasi-harmonic Debye model and the method adopted in the present work is detailed elsewhere in our previous work [2]. The variation of the volume of the unit cell (V) of CuPd versus pressure at temperatures 0, 300 and 600 K is shown in Fig. 8. The volume of the unit cell decreases with increasing pressure at a given temperature. On the other side, as the temperature increases, the volume of the unit cell increases at a given pressure. The rate of increase of V with temperature decreases with increasing pressure.

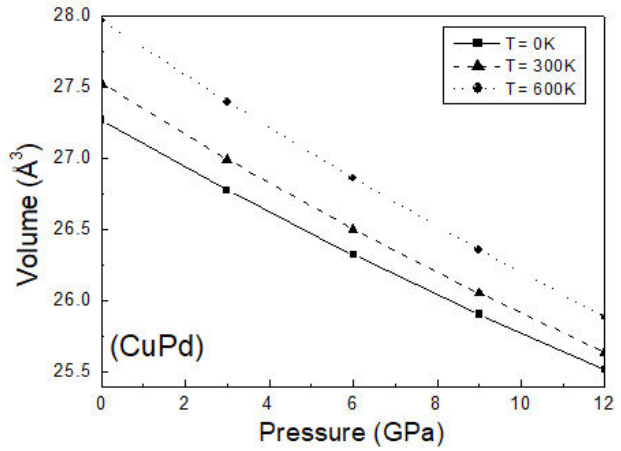

FIGURE 8. Isothermal bulk modulus B_T of CuPd versus pressure at different values of temperature.

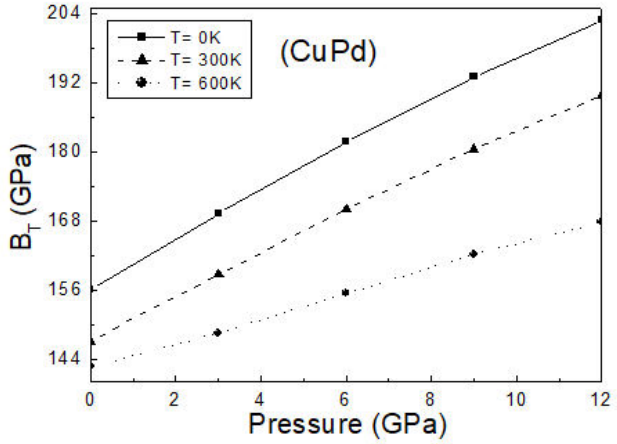

FIGURE 9. Isothermal bulk modulus B_T of CuPd versus pressure at different values of temperature.

The bulk modulus is one of the most important mechanical parameters of the material. It is usually increases as pressure rises [2, 43]. Figure 9 shows the isothermal bulk modulus B_T variation of CuPd compound versus pressure up to 12 GPa at a given temperatures of 0, 300 and 600 K. At zero pressure and room-temperature, the obtained value of the isothermal bulk modulus is around 147.11 GPa. For a given temperature, the bulk modulus B_T increases with increasing pressure, and for a given pressure, the bulk modulus B_T decreases with increasing temperature from 0 to 600 K. This indicates that the material of interest becomes less compressible with increasing pressure. The effect of decreasing temperature and increasing pressure on B_T are nearly the same. We can note that the same trend on the isothermal bulk modulus B_T was also observed in CuSc binary compound [2]. The best fits of our data regarding B_T for CuPd at 0, 300 and 600 K obey the following quadratic expressions, respectively:

$$B_T = 156.0 + 4.69p - 6.40 * 10^{-2}p^2, \quad (12)$$

$$B_T = 147.0 + 4.10p - 4.40 * 10^{-2}p^2, \quad (13)$$

$$B_T = 142.4 + 2.19p - 4.04 * 10^{-3}p^2, \quad (14)$$

where, both B_T and p are expressed in GPa.

The knowledge of the heat capacity of a substance can provide essential insight into its vibrational properties, and it is also mandatory for many applications. From the standard elastic continuum theory, two famous limiting cases are reported. At high temperature, the constant volume heat capacity C_V tends to the Dulong-Petit limit, while at sufficiently low temperature, C_V is proportional to T^3 [44–46]. At intermediate temperatures, however, the temperature dependence of C_V is governed by the details of vibrations of the atoms and for a long time could only be determined from experiments [44]. Figure 10 shows the dependence of the heat capacity C_V on temperature at different pressures (0, 6 and 12 GPa) for the CuPd intermetallic compound with cubic cesium chloride-type structure. From Fig. 10, we can observe that

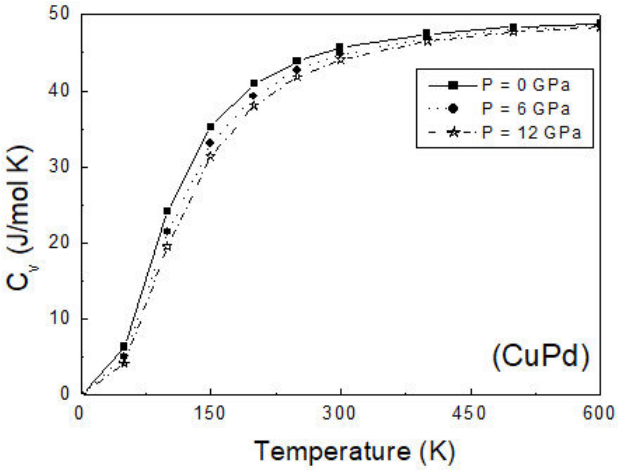

FIGURE 10. Variation of the heat capacity at constant volume as a function of the temperature at various pressures.

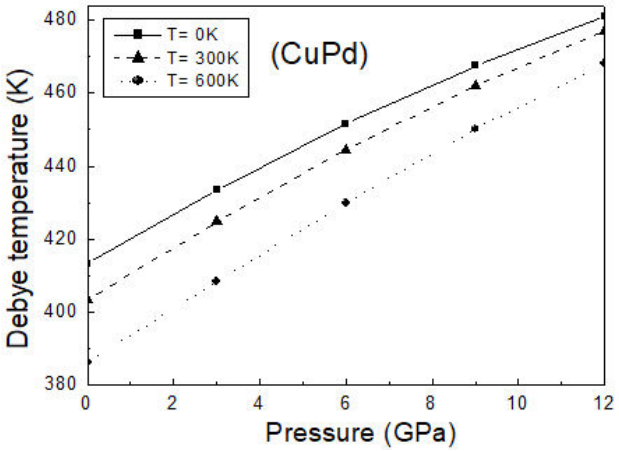

FIGURE 11. Debye temperature of CuPd versus pressure at various temperatures.

the C_V depends on both temperature and pressure, and it increases rapidly with the temperature for $T < 300$ K. At zero-pressure and 300 K, the constant volume heat capacity C_V of CuPd was found to be 45.65 J.mol^{-1}.K^{-1}. It is almost equal to the 45.9 J.mol^{-1}.K^{-1} of CuSc binary compound [2]. For $T > 350$ K, C_V tends to the Dulong-Petit limit. At high temperatures C_V approaches approximately 48.87 J.mol^{-1}.K^{-1} for the material under investigation. As can be seen, the effect of pressure on the heat capacity is not significant. We can note that the same trend on C_V is also observed in CuSc binary compound [2], cubic zinc-blende zirconium carbide material [32], and $Al_{0.25}B_{0.75}As$ semiconducting ternary alloy [44].

Figure 11 shows the [2] dependence of the Debye temperature θ_D on pressure (ranging from 0 up to 12 GPa) at different temperatures (0, 300 and 600 K) for the CuPd intermetallic compound with cubic cesium chloride-type structure. From Fig. 11, we can observe clearly that the θ_D increases monotonically with raising pressure. At a fixed value of pressure, the Debye temperature decreases with increasing

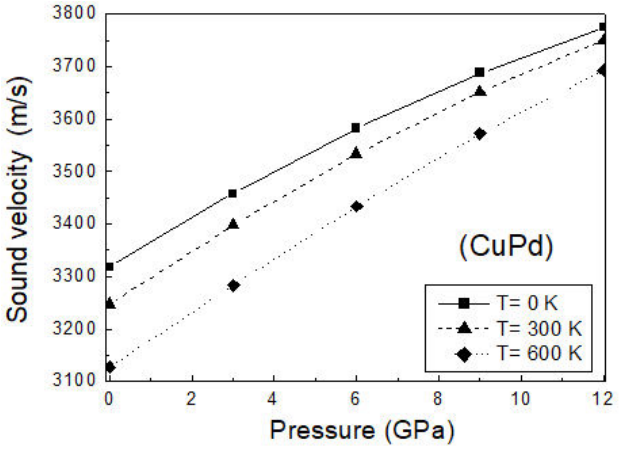

FIGURE 12. Sound velocity versus pressure of CuPd intermetallic compound at different temperatures.

temperature. For CuPd material, the best fits of our data regarding θ_D at 0, 300 and 600 K obey the following quadratic expressions, respectively:

$$\theta_D = 413.24 + 7.14p - 1.25 * 10^{-1}p^2, \quad (15)$$

$$\theta_D = 403.22 + 7.59p - 1.20 * 10^{-1}p^2, \quad (16)$$

$$\theta_D = 386.18 + 7.74p - 0.74 * 10^{-1}p^2, \quad (17)$$

where, θ_D is expressed in K, and p is expressed in GPa. In the Debye model, the sound velocity v_s and the Debye temperature θ_D are related by the following expression [45–47],

$$v_s = k_B\theta_D/\sqrt[3]{6\pi^2\hbar^3 N/V}, \quad (18)$$

where N/V represents the concentration of atoms in the solid.

Figure 12 shows the dependence of the sound velocity v_s at different temperatures (0, 300 and 600 K) for the CuPd intermetallic compound. Such as the Debye temperature, Fig. 12, clearly shows that *vs* increases monotonically with raising pressure. At a fixed value of pressure, v_s decreases with increasing temperature. It can be noted that, a similar trend for the sound velocities versus pressure and temperature was also observed in the case of MgCu intermetallic compound with cubic CsCl-type structure [45], and for aluminum phosphide (AlP) semiconducting compound with cubic zinc-blende phase [46]. For CuPd material, the best fits of our data regarding v_s at 0, 300 and 600 K obey the following quadratic expressions, respectively:

$$v_s = 3317.4 + 50.16p - 9.97 * 10^{-1}p^2, \quad (19)$$

$$v_s = 3246.8 + 53.63p - 9.68 * 10^{-1}p^2, \quad (20)$$

$$v_s = 3126.3 + 55.17p - 8.81 * 10^{-2}p^2, \quad (21)$$

where, v_s is expressed in $m.s^{-1}$ and p is expressed in GPa. In Fig. 13, the variation of the entropy S as a function of temperature at various pressures is presented. At low temperatures, the entropy increases monotonically and very quickly

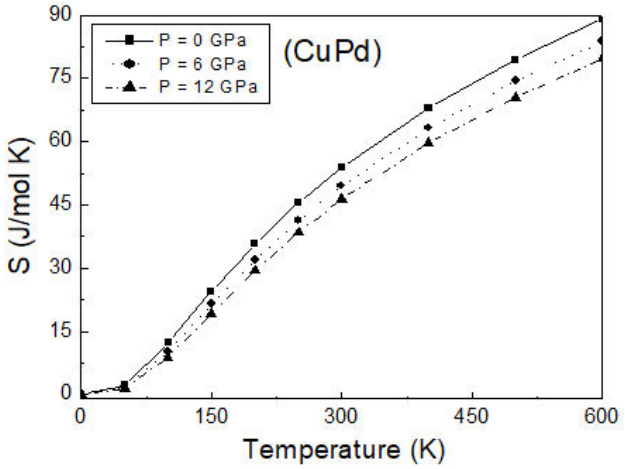

FIGURE 13. Variation of the entropy as a function of temperature at different values of pressure.

with increasing the temperature T. The variation of S as a function of temperature remains qualitatively almost the same as that of pressure ranging from 0 up to 12 GPa. The trend is similar to that of the entropy versus temperature in CuSc material [2], cubic zinc-blende zirconium carbide (ZrC) [32], MgCu [45] intermetallic compound and for cubic zinc-blende AlP semiconducting material [46]. At room-temperature and zero-pressure, the entropy of CuPd is found to be 53.94 J.mol^{-1}.K^{-1}; whereas at pressure of 12 GPa, it is found to be 46.4 J.mol^{-1}.K^{-1}.

4. Conclusions

In conclusion, ab-initio PP-PW method based on the DFT in the GGA approach has been used to investigate the structural, mechanical and thermodynamic properties of CuPd intermetallic compound with the CsCl-type structure at different pressures and temperatures. The calculated equilibrium lattice parameter is in good agreement with the experimental one. Generally, our results of the elastic constants and other derivative quantities were found to be in good agreement with the available theoretical data published in the literature. According to the generalized elastic stability criteria, B2-type structure is mechanically stable up to 26.5 GPa under high-pressure. It is found that pressure influences all thermodynamic parameters of interest in a manner opposite to that of temperature. At zero-pressure and room-temperature, the isothermal bulk modulus was found to be 147.11 GPa; whereas the entropy S was found to be 53.94 J.mol^{-1}.K^{-1}. All features of interest were found to vary monotonically with either temperature or pressure.

1. E. Jain, G. Pagare, S.S. Chouhan and S.P. Sanyal, Structural, electronic, elastic and thermal properties of some transition metal CuX (X=Sc and Pd) intermetallics: A FP-LAPW study, *Comput. Mater. Sci.* **83** (2014) 64, https://doi.org/10.1016/j.commatsci.2013.10.045
2. A. Benmakhlouf, A. Benmakhlouf, O. Allaoui, and S. Daoud, Theoretical study of elastic and thermodynamic properties of CuSc intermetallic compound under high pressure, *Chinese J. Phys.* **57** (2019) 179, https://doi.org/10.1016/j.cjph.2018.11.017.
3. N. Bouarissa, K. Kassali, Mechanical properties and elastic constants of zinc-blende Ga1-xInxN alloys, *Phys. Stat. Sol.* (b) **228** (2001) 663, https://doi.org/10.1002/1521-3951(200112), *Erratum Phys. Stat. Sol.* (b) **231** (2002) 294,
4. N. Bouarissa, Elastic constants and acoustical phonon properties of GaAsxSb1-x, *Mater. Chem. Phys.* **100** (2006) 41, https://doi.org/10.1016/j.matchemphys.2005.12.004.
5. N. Bioud, K. Kassali, N. Bouarissa, Thermodynamic properties of compressed CuX (X=Cl, Br) compounds: Ab initio study, *J. Electron. Mater.* **46** (2017) 2521, https://doi.org/10.1007/s11664-017-5335-x.
6. S. Daoud, N. Bouarissa, N. Bioud, P. K. Saini, High-temperature and high-pressure thermophysical properties of AlP semiconducting material: A systematic ab initio study, *Chem. Phys.* **525** (2019) 110399, https://doi.org/10.1016/j.chemphys.2019.110399.
7. C. C. Rinzler, A. Allanore, A thermodynamic basis for the electronic properties of molten semiconductors: the role of electronic entropy, *Philos. Mag.* **97** (2017) 561, https://doi.org/10.1080/14786435.2016.1269968.
8. S. Saib, N. Bouarissa, P. Rodríguez-Hernández, A. Muñoz, Structural and dielectric properties of AlN under pressure, *Physica B* **403** (2008) 4059, https://doi.org/10.1016/j.physb.2008.08.007.
9. A. Mujica, A. Rubio, A. Muñoz, R. J. Needs, High-pressure phases of group-IV, III-V, and II-VI compounds, *Rev. Mod. Phys.* **75** (2003) 863, https://doi.org/10.1103/RevModPhys.75.863.
10. N. Bouarissa, Electron and positron energy levels and deformation potentials in group-III nitrides, *Phys. Status Solidi B* **231** (2002) 391, https://doi.org/10.1002/1521-3951(200206)231.
11. K. Kassali, N. Bouarissa, Composition and temperature dependence of electron band structure in ZnSe1-xSx, *Mater. Chem. Phys.* **76** (2002) 255, https://doi.org/10.1016/S0254-0584(01)00546-6.
12. K. Daviau, K. K. M. Lee, High-pressure, high-temperature behavior of silicon carbide: *A review, Crystals* **8** (2018) 217, https://doi.org/10.3390/cryst8050217.
13. S. Daoud, N. Bouarissa, Structural and thermodynamic properties of cubic sphalerite aluminum nitride under hydrostatic compression, *Comput. Condens. Matter* **19** (2019) e00359, https://doi.org/10.1016/j.cocom.2018.e00359.

14. N. Bouarissa, Pressure dependence of optoelectronic properties of GaN in the zinc-blende structure, *Mater. Chem. Phys.* **73** (2002) 51, https://doi.org/10.1016/S0254-0584(01)00347-9.

15. F. J. Manjón, D. Errandonea, Pressure-induced structural phase transitions in materials and earth sciences, *Phys. Status Solidi B* **246** (2009) 9, https://doi.org/10.1002/pssb.200844238.

16. N. Bouarissa, Phonons and related crystal properties in indium phosphide under pressure, *Physica B* **406** (2011) 2583, https://doi.org/10.1016/j.physb.2011.03.073.

17. M. A. Baranov, Spherical symmetry of electron shells of atoms and crystal stability, *Elektron. Fiz.-Tekh. Zh.* **1** (2006) 34.

18. Y. Fu, X. Peng, C. Feng, Y. Zhao, Z. Wang, MD simulation of growth of Pd on Cu (111) and Cu on Pd (111) substrates, *Appl. Surf. Sci.* **356** (2015) 651. https://doi.org/10.1016/j.apsusc.2015.08.012.

19. E. Jain, G. Pagare, S. S. Chouhan, S. P. Sanyal, Corrigendum to Structural, electronic, elastic and thermal properties of some transition metal CuX (X = Sc and Pd) intermetallics: A FP-LAPW study [*Comput. Mater. Sci.* **83** (2014) 64] *Comput. Mater. Sci.* **118** (2016) 365. https://doi.org/10.1016/j.commatsci.2016.03.003.

20. E. Jain, G. Pagare, S. Dubey, S. P. Sanyal, Phonon and thermodynamical properties of CuSc: A DFT study, *AIP Conference Proceedings* **1953** (2018) 110033. https://doi.org/10.1063/1.5033058.

21. R. P. Elliott, Constitution of Binary Alloys, 1-2 (McGraw-hill Book Company, New-York, St. Louis, San Fracisco, Toronto, London, Sydney, 1979).

22. https://www.thebalance.com/electrical-conductivity-in-metals-2340117 (written by Terence Bell, updated January 22, 2019).

23. P. Hohenberg, W. Kohn, Inhomogeneous electron gas, *Phys. Rev*. **136** (1964) B864, https://doi.org/10.1103/PhysRev.136.B864.

24. W. Kohn, L. J. Sham, Self-consistent equations including exchange and correlation effects. *Phys Rev B* **140** (1965) A1133, https://doi.org/10.1103/PhysRev.140.A1133.

25. M. D. Segall, P.J.D. Lindan, M.J. Probert, C.J. Pickard, P.J. Hasnip, S.J. Clark, M.C. Payne, First-principles simulation: ideas, illustrations and the CASTEP code, *J. Phys.* **14** (2002) 2717, https://doi.org/10.1088/0953-8984/14/11/301.

26. J.P. Perdew, K. Burke, M. Ernzerhof, Generalized gradient approximation made simple, *Phys. Rev. Lett.* **77** (1996) 3865, https://doi.org/10.1103/PhysRevLett.77.3865.

27. D. Vanderbilt, Soft self-consistent pseudopotentials in generalized eigenvalue formalism, *Phys. Rev. B* **41** (1990) 7892, https://doi.org/10.1103/PhysRevB.41.7892.

28. H.J. Monkhorst, J.D. Pack, Special points for Brillouin-zone integrations, *Phys. Rev. B* **13** (1976) 5188, https://doi.org/10.1103/PhysRevB.13.5188.

29. A. Otero-de-la-Roza, V. Luaña, Gibbs2: A new version of the quasiharmonic model code. II. Models for solid-state thermodynamics, features and implementation, *Comput. Phys. Commun.* **182** (2011) 2232, https://doi.org/10.1016/j.cpc.2011.05.009.

30. F.D. Murnaghan, The compressibility of media under extreme pressures, *Proc. Natl. Acad. Sci. USA.* **30** (1944) 244, https://doi.org/10.1073/pnas.30.9.244.

31. S. Daoud, N. Bioud, N. Lebga, L. Belagraa, R. Mezouar, Pressure effect on structural, elastic and electronic properties of (B3) BSb compound, *Indian J. Phys*, **87** (2013) 355, https://doi.org/10.1007/s12648-012-0231-y.

32. N. R. Rathod, S.K. Gupta, P.K. Jha, First-principles structural, electronic and vibrational properties of zinc-blende zirconium carbide, *Solid State Commun.* **169** (2013) 32, https://doi.org/10.1016/j.ssc.2013.06.011.

33. D. Varshney, G. Joshi, M. Varshney, S. Shriya, *Solid State Sci*, **12** (2010) 864, https://doi.org/10.1016/j.solidstatesciences.2010.02.003.

34. N. Bioud, X-W. Sun, S. Daoud, T. Song, R. Khenata, S. Bin Omran, High-temperature and high-pressure physical properties of CuI with zinc-blende phase by a systematic ab initio investigation, *Optik* **155** (2018) 17, https://doi.org/10.1016/j.ijleo.2017.11.006.

35. S. Daoud, N. Bioud, L. Belagraa, N. Lebga, Elastic, optoelectronic and thermal properties of (B3) BP, *J. Nano- Electron. Phys.*, **5** (2013) 04061,

36. S. Özdemir Kart, A. Erbay, H. Kılıç , T. Cagin, M. Tomak, Molecular dynamics study of Cu-Pd ordered alloys, *Journal of Achievements in Materials and Manufacturing Engineering*, **31** (2008) 41.

37. Md. Zahidur Rahaman, Md. Lokman Ali, Md. Atikur Rahman, Pressure dependent mechanical and thermodynamic properties of newly discovered cubic Na2He, *Chinese J. Phys.* **56** (2018) 231, https://doi.org/10.1016/j.cjph.2017.12.024.

38. S. Daoud, N. Bioud, N. Lebga, Elastic and thermophysical properties of BAs under high pressure and temperature, *Chinese J. Phys.* **57** (2019) 165, https://doi.org/10.1016/j.cjph.2018.11.018.

39. Manal M. Abdus Salam, Theoretical study of CaO, CaS and CaSe via first-principles calculations, *Results in Physics* **10** (2018) 934, https://doi.org/10.1016/j.rinp.2018.07.042.

40. H. Algarni, A. Gueddim, N. Bouarissa, M. A. Khan, H. Ziani, *Res. Phys.* **15** (2019) 102694, https://doi.org/10.1016/j.rinp.2019.102694.

41. B. Ghebouli, M. Fatmi, M.A. Ghebouli, H. Choutri, L. Louail, T. Chihi, A. Bouhemadou, S. Bin-Omran, Theoretical study of the structural, elastic, electronic and optical properties of XCaF3 (X = K and Rb), *Solid State Sci.* **43** (2015) 9, https://doi.org/10.1016/j.solidstatesciences.2015.03.009.

42. Y. Linghu, X. Wu, R. Wang, W. Li, Q. Liu, The Phase Stability, Ductility and Hardness of MoN and NbN: First-Principles Study, *J. Electron. Mater.* **46** (2017) 1914, https://doi.org/10.1007/s11664-016-5258-y.

43. S.U. Rehman, F.K. Butt, F. Hayat, B. Ul Haq, Z. Tariq, F. Aleem, C. Li, An insight into a novel cubic phase SnSe for prospective applications in optoelectronics and clean energy devices, *J. Alloys Compd.* **733** (2018) 22, https://doi.org/10.1016/j.jallcom.2017.10.192.

44. H. Algarni, O. A. Al-Hagan, N. Bouarissa, M. A. Khan, T. F. Alhuwaymel, Dependence on pressure of the elastic parameters and microhardness of InSb, *Infrared Phys. Technol.* **86** (2017) 176, https://doi.org/10.1016/j.infrared.2017.09.012.

45. K. Boubendira, H. Meradji, S. Ghemid, F. El Haj Hassan, Theoretical prediction of the structural, electronic, and thermal properties of Al1-xBxAs ternary alloys, *Mater. Sci. Semicond. Process.* **16** (2013) 2063, https://doi.org/10.1016/j.mssp.2013.07.022.

46. S. Daoud, N. Bioud, P. K. Saini, Finite temperature thermophysical properties of MgCu intermetallic compound from quasi-harmonic Debye model, *J. Magnes. Alloys*, **7** (2019) 335, https://doi.org/10.1016/j.jma.2019.01.006.

47. S. Daoud, N. Bioud, N. Bouarissa, Structural phase transition, elastic and thermal properties of boron arsenide: Pressure-induced effects, *Mater. Sci. Semicond. Process.* **31** (2015) 124, https://doi.org/10.1016/j.mssp.2014.11.024.

48. K.W. Böer, U.W. Pohl, Semiconductor Physics, Springer International Publishing AG, Switzerland, 2018.

49. N. Lebga, S. Daoud, X-W Sun, N. Bioud, A. Latreche, Mechanical and thermophysical properties of cubic rock-salt AlN under high pressure, *J. Electron Mater.*, **47**, (2018) 3430, https://doi.org/10.1007/s11664-018-6169-x.

50. S. Amari, S. Daoud, Structural phase transition, elastic constants and thermodynamic properties of TmAs: An ab-initio study, *Comput. Condens. Matter*, **33** (2022) e00764. https://doi.org/10.1016/j.cocom.2022.e00764.